

Three-Dimensional $\{\text{Co}^{3+}-\text{Zn}^{2+}\}$ and $\{\text{Co}^{3+}-\text{Cd}^{2+}\}$ Networks Originated from Carboxylate-rich Building Blocks: Syntheses, Structures, and Heterogeneous Catalysis

Girijesh Kumar and Rajeev Gupta*

Department of Chemistry, University of Delhi, Delhi 110 007, India

Supporting Information

ABSTRACT: The present work shows the utilization of Co^{3+} complexes appended with either *para*- or *meta*-arylcarboxylic acid groups as the molecular building blocks for the construction of three-dimensional $\{\text{Co}^{3+}-\text{Zn}^{2+}\}$ and $\{\text{Co}^{3+}-\text{Cd}^{2+}\}$ heterobimetallic networks. The structural characterizations of these networks show several interesting features including well-defined pores and channels. These networks function as heterogeneous and reusable catalysts for the regio- and stereoselective ring-opening reactions of various epoxides and size-selective cyanation reactions of assorted aldehydes.



INTRODUCTION

The construction of extended networks from molecular building blocks is of great importance due to their ability to place molecular components at desired architectural forms.¹ The use of discrete molecular building blocks further controls the speciation and coordination environments within the extended network.² The utilization of extended networks as heterogeneous catalysts for various organic transformation reactions has shown promising results due to the optimized control of free space available within such microporous materials.³ Such catalytic properties are largely responsible due to the crystalline nature of these networks and the occurrence of well-defined pores and channels for the better substrates/reagents accessibility to the catalytic sites.^{3a,b} For catalytic applications, it is important that the catalytic metal ions are either coordinately unsaturated or ligated by easily dissociable/replaceable solvent molecules. Further, it is also desirable to design a material in such a way so as to circumvent or at least minimize the catenation which prevents accessibility of the substrate and/or reagents.⁴ A combination of all such desired features is often challenging to incorporate in traditional solid catalysts such as zeolites or metal-organic frameworks (MOFs). However, utilization of a well-defined coordination complex as the building block controls several of the mentioned parameters and therefore has become a well-followed area of research.

Our research group has been working on developing coordination complexes as the building blocks for the construction of ordered structures.^{5,6} These building blocks offer either hydrogen bond (H-bond)⁵ or coordination sensitive functional groups^{6c-g} to generate highly ordered two- (2D) and three-dimensional (3D) networks. Notably, such an approach offers precise control on the placement of primary and secondary (often catalytic) metal ions with an identical chemical environment due to material's highly crystalline nature. Moreover, this approach was also successful in avoiding catenation completely. These points have helped us in developing assorted catalytic

systems which have displayed substrate-specific,^{6a,b} regio- and stereoselective,^{6b-f} and very recently size-selective catalytic reactions.^{6g}

Assorted ligands as well as the molecular building blocks containing carboxylic acid groups are among the most extensively investigated synthons for generating interesting and robust networks including MOFs.⁷ Recent examples of such networks have focused on the development of functional materials that are capable of gas storage,⁸ light harvesting,⁹ catalysis,¹⁰ proton conduction,¹¹ chemical sensing,¹² drug delivery,¹³ and luminescent materials.¹⁴ A carboxylic acid group not only provides a unique coordination mode but also affords stable architectures often necessary for subsequent applications. Herein, we report the syntheses, structures, and properties of $\{\text{Co}^{3+}-\text{Zn}^{2+}\}$ and $\{\text{Co}^{3+}-\text{Cd}^{2+}\}$ networks using Co^{3+} -complexes appended with *para*- and *meta*-arylcarboxylic acid as the building blocks. We display that our approach has resulted in the construction of noncatenated highly ordered 3D architectures with well-defined pores and channels that are lined with catalytic metal ions. Furthermore, we show the heterogeneous catalytic application of such 3D architectures in the ring-opening reactions (RORs) of various epoxides and cyanation reactions (CRs) of assorted aldehydes under solvent-free conditions. Our results show a precise control over the stereoselectivity, regioselectivity, and size-selectivity that has been related to the unique structural features offered by these heterobimetallic networks.

EXPERIMENTAL SECTION

Materials and Methods. Commercially available reagents of analytical grade were used as received without further purification. Solvents were purified using the standard literature procedure.^{15a} The building blocks $\text{Et}_4\text{N}[\text{Co}(\text{L}^{\text{p-COOH}})_2]$ **1** and $\text{Et}_4\text{N}[\text{Co}(\text{L}^{\text{m-COOH}})_2]$ **2** (where $\text{H}_2\text{L}^{\text{p-COOH}} = 2,6\text{-bis}(4\text{-benzoic acid-carbonyl})\text{pyridine}$;

Received: March 2, 2013

Published: September 17, 2013

Table 1. Crystallographic Data Collection and Structure Refinement Parameters for Networks 3–6

	3	4	5	6
empirical formula	C ₈₄ H ₉₄ N ₁₂ O _{49.5} Co ₂ Zn ₆	C ₄₂ H ₅₇ CoN ₆ O ₃₀ Zn ₃	C ₈₄ H ₉₄ Cd ₄ Co ₂ N ₁₂ O ₆₅	C ₈₄ H ₉₄ Cd ₅ Co ₂ N ₁₂ O ₄₉
fw	2573.90	1381.03	2879.27	2735.61
T (K)	150(2)	298(2)	150(2)	298(2)
cryst syst	triclinic	triclinic	orthorhombic	monoclinic
space group	$P\bar{1}$	$P\bar{1}$	<i>Pnma</i>	$P2_1/c$
a (Å)	16.082(5)	11.361(5)	19.018(5)	13.154(5)
b (Å)	17.074(5)	15.862(5)	29.527(5)	39.417(5)
c (Å)	27.878(5)	16.279(5)	23.963(5)	19.290(5)
α (deg)	92.586(5)	73.758(5)	90	90
β (deg)	105.969(5)	89.749(5)	90	91.837(5)
γ (deg)	117.000(5)	79.948(5)	90	90
V (Å ³)	6427(3)	2770.2(17)	13456(5)	9997(5)
Z	1	2	4	4
d (g cm ⁻³)	1.304	1.621	1.396	1.806
μ/mm ⁻¹	1.432	1.674	0.954	1.471
F(000)	2524	1358	5592	5400
goodness-of-fit (F ²)	0.938	1.056	1.064	1.063
R(int)	0.0809	0.0393	0.0208	0.0885
R ₁ , wR ₂ [I > 2σ(I)]	0.0903, 0.2194	0.0530, 0.1540	0.0791, 0.2109	0.0659, 0.1481
R ₁ , wR ₂ (all data) ^a	0.1354, 0.2460	0.0772, 0.1715	0.0918, 0.2270	0.0875, 0.1621

$$^a R_1 = \frac{\sum ||F_o| - |F_c||}{\sum |F_o|}; wR_2 = \left\{ \frac{\sum [w(|F_o|^2 - |F_c|^2)]}{\sum [wF_o^4]} \right\}^{1/2}.$$

H₂L^{m-COOH} = 2,6-bis(3-benzoicacid-carbonyl)pyridine) were synthesized as per our recent report.^{5b}

Synthesis of [(1)₂Zn₆(OH)₂(H₂O)₁₀·14H₂O]_n (3). Network 3 was synthesized by layering a methanol solution of complex 1 (100 mg, 1.004 mmol, 6 mL) over an aqueous solution of Zn(OAc)₂·2H₂O (66.89 mg, 2.510 mmol, 2 mL) with an intermediate layer of *tert*-butyl alcohol (1 mL) in a glass tube of 75 mm with an ID of 7.5 mm. After a period of 6–7 days, deep green colored crystals of network 3 were deposited, which were collected, washed with CH₃OH, and dried under a vacuum. Yield (based on 1): 0.208 g (81%). Anal. Calcd. for C₈₄H₇₄Zn₆Co₂N₁₂O₃₆·14H₂O: C, 38.95%; H, 3.97%; N, 6.49%; Found: C, 39.14%; H, 4.35%; N, 6.54%. FTIR spectrum (KBr disc, selected peaks): 3422 (OH), 1605 (COO) cm⁻¹. Absorption spectrum (solid state, λ_{max}/nm): 640, 560, 480.

Synthesis of [(2)Zn₃(OH)(H₂O)₆·11H₂O]_n (4). Network 4 was prepared in a similar manner with a similar scale as that of network 3, however, using complex 2 in place of complex 1. Reddish green colored crystals of 4 were collected after a period of 4–5 days. Yield (based on 2): 0.218 g (85%). Anal. Calcd. for C₈₄H₇₈Zn₆Co₂N₁₂O₃₈·11H₂O: C, 39.23%; H, 3.97%; N, 6.54%; Found: C, 39.49%; H, 4.44%; N, 6.61%. FTIR spectrum (KBr disc, selected peaks): 3405 (OH), 1577 (COO, C=O) cm⁻¹. Absorption spectra (solid state, λ_{max}/nm): 620, 555, 460.

Synthesis of [(1)Cd_{2.5}(H₂O)₁₀·24H₂O]_n (5).^{6g} Network 5 was synthesized by treating a solution of Cd(OAc)₂·2H₂O (66.89 mg, 2.510 mmol) in CH₃OH (2 mL) with a solution of complex 1 (100 mg, 1.004 mmol) in CH₃OH (5 mL). The reaction mixture was stirred at room temperature for 1 h. A brownish yellow colored product was precipitated, which was collected, washed with methanol, and dried under a vacuum. The crude product thus obtained was redissolved in water, filtered, and layered with *tert*-butyl alcohol in a glass tube of 75 mm with an ID of 7.5 mm at room temperature. After a period of 3–4 days, brown-colored crystals of network 5 were obtained. Yield (based on 1): 0.225 g (78%). Anal. Calcd. for C₈₄H₇₂Cd₅Co₂N₁₂O₃₄·24H₂O: C, 34.72%; H, 4.16%; N, 5.78%; Found: C, 34.95%; H, 4.23%; N, 5.81%. FTIR spectrum (KBr disc, selected peaks): 3423 (OH), 1605 (COO), 1585 (C=O) cm⁻¹. Absorption spectrum (solid state, λ_{max}/nm): 635, 560, 495.

Synthesis of [(2)Cd_{2.5}(H₂O)₁₅·9H₂O]_n (6).^{6g} Network 6 was prepared in a similar fashion with a similar scale as that of network 5, however, using complex 2. Reddish brown colored crystals of network 6 were obtained after a period of 5–6 days. Yield (based on 2): 0.238 g (87%). Anal. Calcd. for C₈₄H₈₂Cd₅Co₂N₁₂O₃₉·9H₂O: C, 37.01%; H, 3.70;

N, 6.17; Found: C, 36.96%; H, 3.39%; N, 6.16%. FTIR spectrum (KBr disc, selected peaks): 3422 (OH), 1561 (COO, C=O) cm⁻¹. Absorption spectrum (solid state, λ_{max}/nm): 622, 570, 499.

General Procedure for the Ring-Opening Reactions of Epoxides. The ring-opening reactions of the epoxides were carried out under ambient conditions. In a typical aminolysis reaction, cyclohexeneoxide (0.495 mmol) was treated with aniline (0.495 mmol) in the presence of catalyst 3, 4, 5, or 6 (0.0098 mmol). However, in the case of styrene oxide, 0.438 mmol of epoxide was treated with 0.438 mmol of aniline in the presence of 0.00875 mmol of catalyst. The reaction was monitored by the thin-layer chromatography (TLC). After 4 h, 2 mL of EtOAc was added to the reaction mixture, and the solid catalyst was filtered off. The filtrate was concentrated under the reduced pressure. The crude product was purified by flash column chromatography on silica gel using hexane/ethyl acetate mixture (5:1) as the eluent. The products were isolated, quantified, and analyzed by GC/GC–MS techniques. The recovered catalyst was washed with diethyl ether, dried, and reused without further purification or regeneration. Moreover, in several cases the recovered catalyst was characterized by the X-ray powder diffraction (XRPD) and FTIR spectra that showed identical results to that of freshly prepared samples.

General Procedure for the Cyanosilylation Reaction of Aldehydes. The cyanosilylation reactions of aldehydes were carried out under ambient conditions. In a typical cyanosilylation reaction, 5 mol % catalyst (3, 4, 5, or 6) was added to a mixture of aldehyde (1 mmol) and (CH₃)₃SiCN (5 mmol). The resulting mixture was stirred at room temperature, and progress of the reaction was monitored by TLC. After completion of the reaction, 2 mL of EtOAc was added to the reaction mixture, and the solid catalyst was filtered off. The filtrate was concentrated under reduced pressure. The crude product was purified by flash column chromatography on silica gel using 10% ethyl acetate/hexane mixture as the eluent. The products were isolated, quantified, and analyzed by GC/GC–MS techniques.

Physical Methods. The FTIR spectra (KBr disk, 4000–400 cm⁻¹) were recorded either with Perkin-Elmer FTIR 2000 or Spectrum-Two spectrometers. The NMR spectroscopic measurements were carried out with a Jeol 400 MHz spectrometer with TMS as the internal standard. The solution absorption and diffused reflectance spectra were recorded with Perkin-Elmer Lambda 25 and Lambda 35 spectrophotometers, respectively. The elemental analysis data were obtained with an Elementar Analysen Systeme GmbH Vario EL-III instrument. GC–MS studies were performed with a Shimadzu instrument (QP 2010)

Scheme 1. Synthetic Routes for Networks 3–6

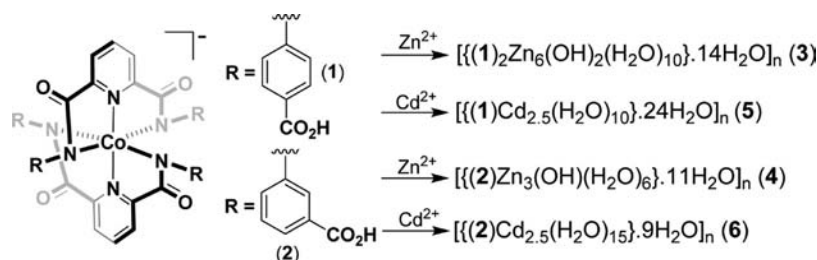


Table 2. Selected Ranges for the Bond Distances (Å) Observed for Networks 3–6

bond lengths	3	4	5	6
Co1–N _{pyridine}	1.851–1.881	1.847–1.859	1.859–1.860	1.840–1.855
Co1–N _{amide}	1.923–1.984	1.939–1.962	1.950–1.979	1.949–1.970
M–O _{carboxylate}	1.961–2.474	2.088–2.326	2.295–2.525	2.323–2.549
M–O _{bridging carboxylate}	1.961–2.093	2.015–2.171		2.159–2.459
M–O _{oxo}	2.111–2.123	2.010–2.077		
M–O _{bridging water}	2.255–2.289			
M–O _{terminal water}	1.903–2.172	2.010–2.229	2.263–2.582	2.194–2.459

with an RTX-5SIL-MS column. The nitrogen sorption isotherms were measured with an AUTOSORB-1C, Quantachrome (USA) instrument in a standard volumetric technique, at 77 K. Under continuous adsorption conditions; prior to measurements, samples were heated at 350 °C for 12 h with helium gas used for flushing purpose. A part of the N₂ sorption isotherms in the P/P_0 range was fitted to the Brunauer–Emmett–Teller (BET) equation to determine the BET surface area. For the Langmuir surface area, data from the whole adsorption isotherm were used. Thermal gravimetric analysis (TGA) and differential scanning calorimetry (DSC) were performed with DTG 60 Shimadzu and TA-DSC Q200 instruments, respectively, at 5 °C min⁻¹ heating rate under the nitrogen atmosphere. The X-ray powder diffraction (XRPD) studies were performed either with an X'Pert Pro from Panalytical or a Bruker AXS D8 Discover instrument (Cu K α radiation, $\lambda = 1.54184$ Å). The samples were ground and subjected to the range of $\theta = 5$ –30° with a scan rate of 1–0.72°/min at room temperature.

Crystallography. The details for the single crystal X-ray diffraction data collection and structure solution for networks 3–6 are provided in the Supporting Information. Table 1 contains the crystallographic and structure solution parameter for networks 3–6. The CIF files for networks 5 and 6 have been included in our previous communication.^{6g}

RESULTS AND DISCUSSION

Synthesis and Characterization. The building block complexes Et₄N[Co(L^{p-COOH})₂] (1) and Et₄N[Co(L^{m-COOH})₂] (2) offer four uncoordinated arylcarboxylic acid groups.^{5b} Such appended arylcarboxylic acid groups on reaction with secondary metal ions provided the desired networks 3–6 (Scheme 1). In each case, the reaction with secondary metal resulted in a distinct color change from deep green to brownish-yellow or reddish-brown. Networks 3–6 exhibited strong bands between 1605–1577 cm⁻¹ due to the ν_{COO} stretches in their FTIR spectra.^{15b} In addition, broad features between 3400–3430 cm⁻¹ were indicative of the presence of coordinated as well as lattice water molecules.^{15b} Networks 3–6 displayed the λ_{max} in the range of 620–640 nm in their diffused reflectance spectra which are tentatively assigned to the d–d transition in the Co³⁺ ion of the building block core (Figures S1 and S2, Supporting Information, SI). The XRPD patterns of the freshly prepared samples of networks 3–6 were nearly identical to those simulated from the single-crystal structures indicative of phase purity of the bulk samples (Figures S3–S6, SI).

Crystal Structures. All four heterobimetallic networks were characterized by the single-crystal X-ray diffraction studies to understand the network generation via the mediation of building blocks. For all four networks, Table 2 provides the range observed for the bond distances, whereas Tables S1–S4 (Supporting Information) contain the detailed bonding parameters.

Both networks 3 and 4 crystallized in the triclinic cell system with $P\bar{1}$ space group. The molecular structures of networks 3 and 4 are quite similar and show that the central Co³⁺ ion is meridionally coordinated by two tridentate ligands. The octahedral Co³⁺ ion is bonded to four N_{amide} atoms in the basal plane and two N_{pyridine} atoms in the axial position (Figures 1a and 2a). The Co–N_{amide} bond distances are found to be longer than the Co–N_{pyridine} distances (Table 2). Two axial pyridine rings are trans to each other with the bond angle in excess of 178°. The diagonal N_{amide} groups make angle with the Co³⁺ ion close to 163° in both cases.

The unit cell of network 3 contains 2 building blocks, 6 Zn²⁺ ions, 2 bridging hydroxide, 1 bridging and 9 coordinated water, and 14 uncoordinated water molecules. The molecular structure of network 3 shows that the Co³⁺-based building blocks are connected through Zn²⁺ ions (Figure 1). Every building block offers four *para*-arylcarboxylate groups, and each one assists in coordinating five different Zn²⁺ ions. The five-coordinate Zn1 ion is ligated to four O_{carboxylate} atoms and a hydroxide group (O13), which further bridges Zn2 and Zn3 ions. The six-coordinate Zn2 ion is connected to three O_{carboxylate} atoms, two bridging hydroxide groups (O13 and O27), and a bridging aqua group (O14). The Zn3 is also six-coordinated with two O_{carboxylate} atoms and two bridging oxygen atoms (O13_{hydroxide}, O14_{aqua}), while the remaining sites are occupied by the water molecules. The four-coordinate Zn4 ion is ligated to three O_{carboxylate} atoms and a hydroxide ion (O27), which further bridges Zn2 and Zn5 atoms. For the five-coordinate Zn5 ion, the basal-plane is constituted by three O_{carboxylate} atoms and a bridging O27_{hydroxide} atom, whereas the apical site is satisfied by a water molecule.

Notably, one of the Zn²⁺ ions, Zn6, is present in the crystal lattice as a Zn(H₂O)₆ cluster. The Zn(H₂O)₆ cluster is trapped within the crystal lattice with the help of strong H-bonds between O_{amide} atoms and Zn6-bound water molecules (Table S4, SI). It is

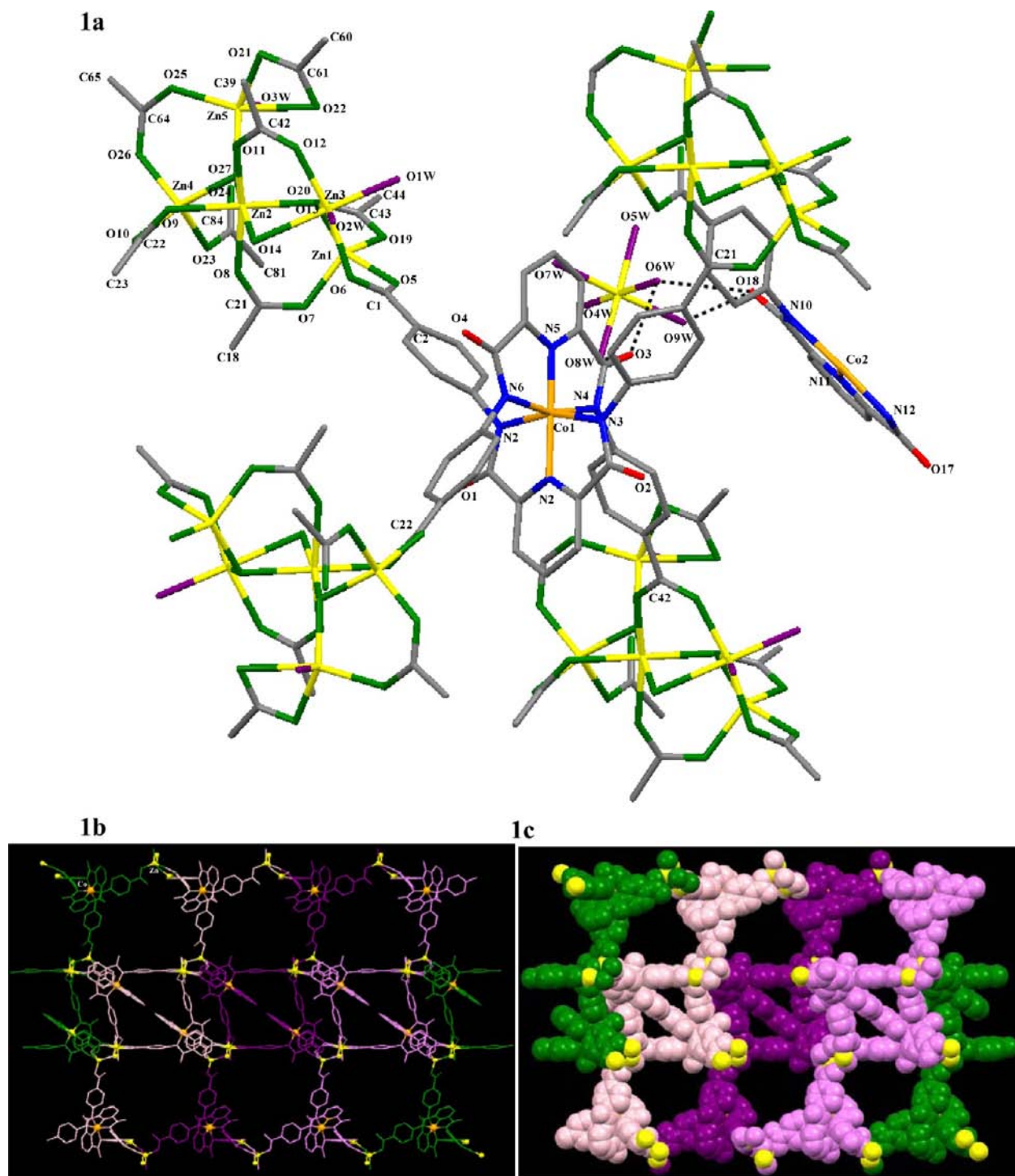


Figure 1. (a) Stick representation of a selected part of the crystal structure of network 3. Color code: orange, Co; yellow, Zn; blue, N; green, O_{carboxylate}; purple, O_{water}; red, O_{amide}; gray, C. (b) Packing diagram in a view along the *a*-axis. (c) Space-filling view along the *a*-axis showing pores and channels in the structure of network 3; the coordinated water molecules are omitted for clarity to show accessible Lewis acidic Zn²⁺ ions (yellow spheres).

important to mention that this Zn(H₂O)₆ cluster does not come out from the crystal lattice even when the powdered sample is suspended in various solvents. Further, when the powdered network is suspended in solution containing several other metal ions, no exchange was noticed even after 72 h. These experiments suggest the stable nature of Zn(H₂O)₆ cluster within the network. The presence of Zn(H₂O)₆ cluster appears to be driven by the requirement of charge balance.

The unit cell of network 4 contains 1 building block, 3 Zn²⁺ ions, 1 hydroxide group, 6 coordinated and 11 uncoordinated water molecules. Here, a 2D layer structure is generated via coordination between Zn²⁺ ions and arylcarboxylate fragments that are originated from different building blocks (Figure 2a,c). Out of three Zn²⁺ ions, two are six-coordinate (Zn1, Zn2), whereas the third one (Zn3) displays a five-coordinate geometry. A μ_3 -hydroxide group bridges all three zinc atoms. The Zn1 forms bond with five O_{carboxylate} atoms, while the sixth site is

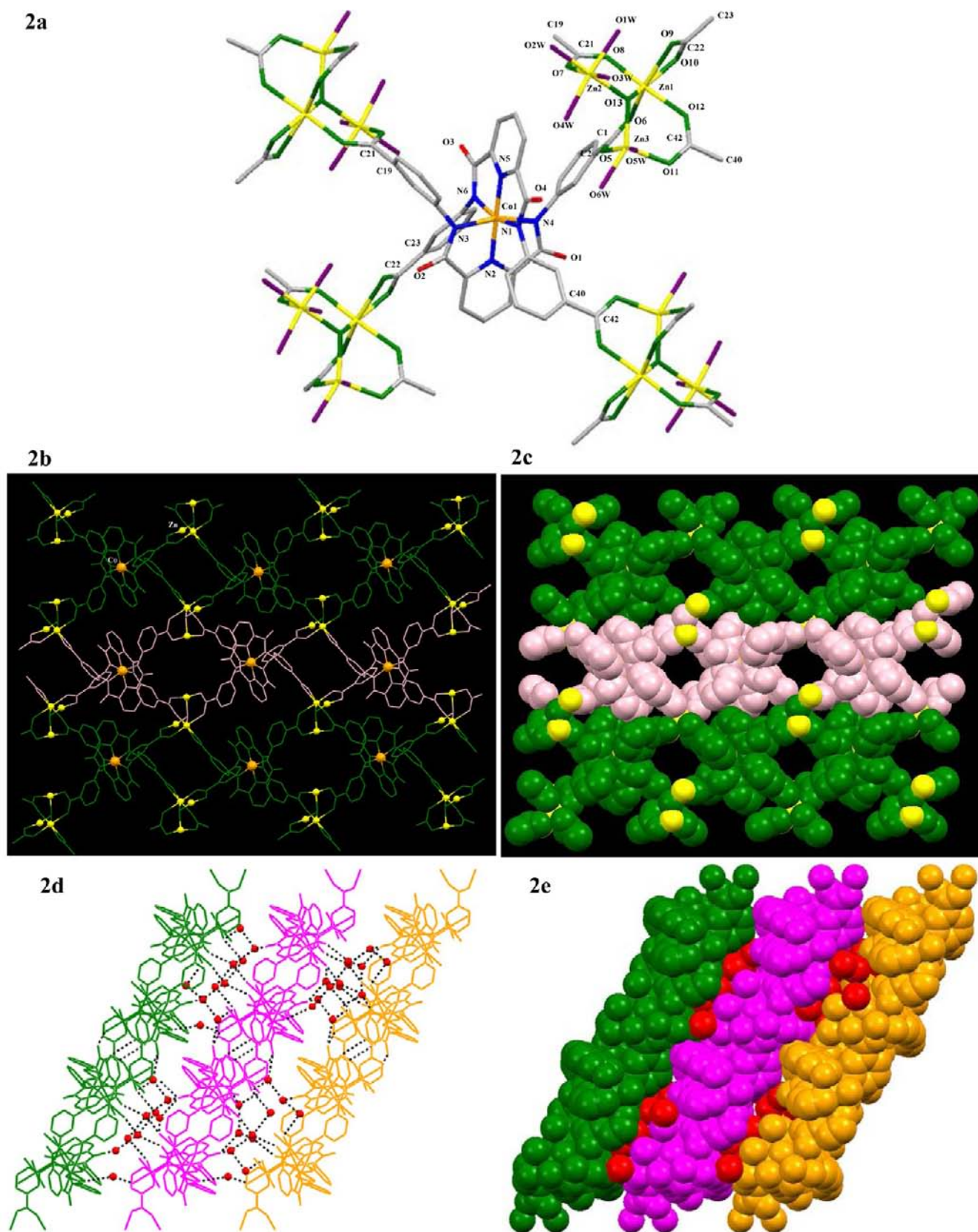


Figure 2. (a) Stick representation of a selected part of the crystal structure of network 4. Color code: orange, Co; yellow, Zn; blue, N; green, O_{carboxylate}; purple, O_{water}; red, O_{amide}; gray, C. (b) Packing diagram in a view along the *a*-axis. (c) Space-filling view along *a*-axis showing pores and channels in the structure of network 4; the coordinated water molecules are omitted for clarity to show accessible Lewis acidic Zn²⁺ ions (yellow spheres). Panels (d) and (e) showing layered structure where individual layers are connected through water molecules (red spheres) via H – bonds (shown by black dots).

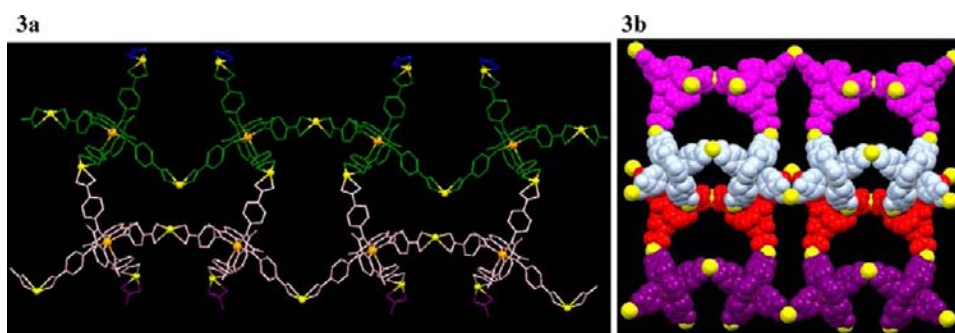


Figure 3. (a) A selected part of the crystal structure of network **5** in a view along the *a*-axis. (b) Space-filling view along the *a*-axis showing pores and channels; the coordinated water molecules are omitted for clarity to show accessible Lewis acidic Cd^{2+} ions (yellow spheres).

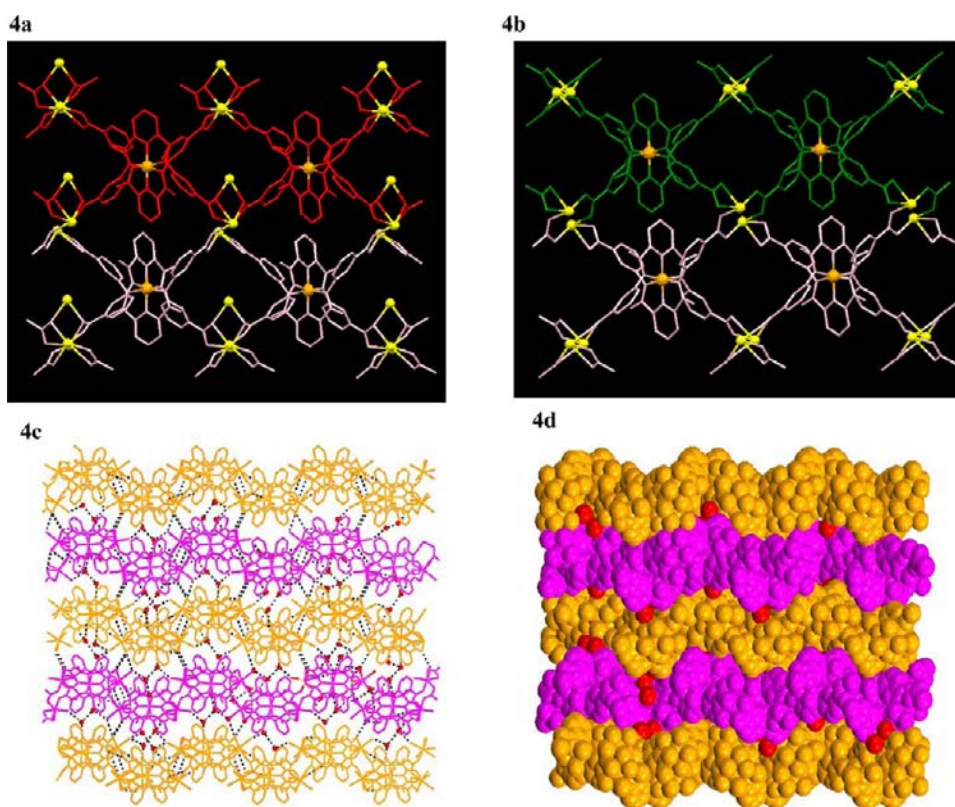


Figure 4. In a view along the *a*-axis showing a selected part of the crystal structure of network (a) **6a** and (b) **6b**; the coordinated water molecules are omitted for clarity to show accessible Lewis acidic Cd^{2+} ions (yellow spheres). Panels (c) and (d) show a layered structure where individual layers are connected through water molecules (red spheres) via H-bonds (shown by black dots).

satisfied by a bridging hydroxide group ($\text{O}13$). Similarly, the $\text{Zn}2$ ion is coordinated to $\text{O}7_{\text{carboxylate}}$, $\text{O}13_{\text{hydroxide}}$, and four water molecules. The $\text{Zn}3$ ion is coordinated to two $\text{O}_{\text{carboxylate}}$ atoms, while the remaining sites are occupied by a bridging $\text{O}13_{\text{hydroxide}}$ and two water molecules. Notably, network **4** is a layered material where 2D layers are stacked through water molecules (shown as red spheres in Figure 2d,e). The layers are held together via H-bonds between O_{amide} groups and coordinated and uncoordinated water molecules ($\text{O}_{\text{amide}}\cdots\text{O}_{\text{water}}$ separations: 2.584–2.952 Å).

As noted for **3** and **4**, both $\{\text{Co}^{3+}-\text{Cd}^{2+}\}$ based networks **5**^{6g} and **6**^{6g} displayed similar structure where Co^{3+} -based building blocks are connected through Cd^{2+} ions. The unit cell in each case consists of one building block, 2.5 Cd^{2+} ions, and several coordinated and uncoordinated water molecules. In both cases, every building block offers four arylcarboxylate fragments which

coordinate different Cd^{2+} ions. Such an arrangement results in the generation of $\{\text{Co}^{3+}-\text{Cd}^{2+}\}$ based networks (Figures 3, 4 and S7, S8 in SI). Importantly, network **6** is a layered material as also noted for network **4**. Here, individual 2D layers (shown in orange for **6a** and pink color for **6b**, Figure 4c,d) are connected to each other via an array of H-bonds involving $\text{O}_{\text{carboxylate}}$, O_{amide} , coordinated, and uncoordinated water molecules ($\text{O}\cdots\text{O}$ separations: 2.713–2.827 Å).

Although all four networks show assorted molecular structures, interestingly however, topologically, all four are quite similar.^{16a,b} For example, all four networks offer secondary building units (SBUs) which are composed of Zn^{2+} or Cd^{2+} ions coordinated by a certain number of arylcarboxylic acid fragments: $\text{Zn}_5(\text{COO})_8$ (**3**); $\text{Zn}_3(\text{COO})_4$ (**4**); $\text{Cd}(\text{COO})_2$ (**5**); $\text{Cd}_3(\text{COO})_4$ (**6a**); and $\text{Cd}_2(\text{COO})_4$ (**6b**).^{16a,b} The assorted SBUs are expanded through the tetra-connected cobalt-based

building blocks to generate the extended networks.^{16c} Thus, **3** is composed of octagonal SBUs expanded to a 4,8-connected network through Co-based tetra-connected nodes. Similarly, network **4** may be viewed as 4,4-connected network via tetrahedral SBUs and Co-based nodes, whereas network **5** shows 4,2-connected network. On the other hand, both networks **6a** and **6b** are composed of tetrahedral SBUs and tetra-connected Co-based nodes.

All networks show solvent-accessible voids (SAVs) of different volume, and a noticeable difference was found between the networks created by *para*- versus *meta*-arylcarboxylic acid based building blocks. For example, the crystal structures of networks **3** and **5** (both with *para*-arylcarboxylic acid groups) showed SAVs of volume 1861 Å³ and 2637.5 Å³, respectively. These numbers correspond to 29% and 20% of the unit cell volume for networks **3** and **5**, respectively. On the other hand, networks **4** and **6** (both with *meta*-arylcarboxylic acid groups) offered only 2.3% and 0.3% SAVs per unit cell volume. This difference is due to a highly symmetrical nature of bonding between the *meta*-appended arylcarboxylate groups to that of metal ions (packing behavior) in the case of networks **4** and **6** that has resulted in very small voids within the lattice. In fact, a very similar H-bonding based packing was observed for the Co³⁺-based metalloligands appended with *meta*-arylcarboxylic acid groups offering very small SAVs.^{5b}

All four heterobimetallic networks possess several interesting structural features. For example, all four networks showed the presence of well-defined pores and channels within the microporous network. These channels were found to contain lattice water molecules which are held together by weak H-bonding interactions. Interestingly, both networks **3** and **5** with *para*-arylcarboxylic acid groups offer two types of pores with cross sections of 12.5 × 9.9 and 17.4 × 14.7 Å² (for **3**) and 17.9 × 16.3 and 21.5 × 7.5 Å² (for **5**), respectively.¹⁷ It is important to note that both these networks also offered largest SAVs. In contrast, networks **4** and **6** (both **6a** and **6b**) with *meta*-arylcarboxylic acid groups were densely packed (thus offered little SAVs) and only presented a single channel opening: 11.9 × 10.3 Å² (for **4**), and 13.6 × 10.4 (for **6a**) and 11.0 × 10.9 (for **6b**). Therefore, it could be concluded that the *para*-arylcarboxylic acid groups result in an elongated network that generate wider pores and offer large SAVs. Such structural features are expected to enhance the substrate/reagent accessibility. On the other hand, the layered structural nature for networks **4** and **6** suggests plausible substrate/reagent intercalation despite densely packed 2D layers. Further, all networks showed the orderly arrangement of secondary metals within the crystalline structure. Importantly, these secondary metals are not only Lewis acidic in nature but are also coordinated with a large number of labile water molecules. Therefore, it was presumed that the suitable O-based substrates may interact with the Lewis acidic sites and replace the labile water molecules without altering the network topology, and such a situation may assist in possible organic transformations (vide infra).

■ THERMAL PROPERTIES

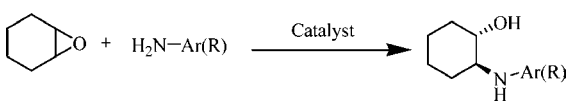
Thermal profiles of coordination networks are necessary as many applications depend on their thermal stability. In the present work, all networks were found to have a large number of coordinated as well as lattice water molecules, and it was important to analyze the fate of these water molecules so as to ascertain their role in the structural integrity. Therefore, thermal gravimetric analysis (TGA) and differential scanning calorimetric (DSC) analyses were performed on all heterobimetallic networks

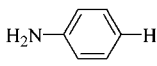
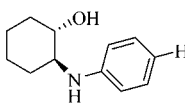
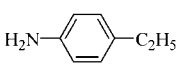
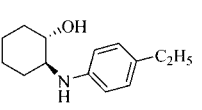
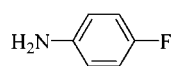
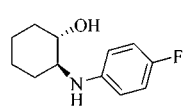
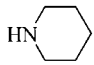
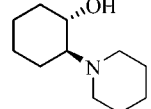
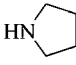
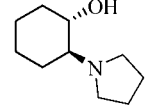

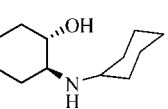
(Figures S9–S12, SI). All four networks show a very similar thermal profile owing to a similar network structure. In all four cases, the first weight loss was due to the liberation of both coordinated and uncoordinated water molecules. Such a weight loss was noticed from ambient temperature to ca. 180 °C in the form of a close match between the observed and calculated values. For network **3**, the observed and calculated weight losses were 16.50 and 16.68% for the loss of 24 (10 coordinated and 14 uncoordinated) water molecules. In a similar manner, network **4** showed observed weight loss of 12.06% (calcd. 11.90%) for the loss of 17 water molecules. For network **5**, the weight loss (obsd/calcd (%); 21.11/21.26) corresponded to the liberation of 10 coordinated and 24 uncoordinated water molecules. Similarly, network **6** also showed the weight loss due to 24 water molecules (obsd/calcd (%); 15.44/15.79). All four networks were stable after the loss of coordinated as well as lattice water molecules and did not show further weight loss up to ca. 350 °C. However, when the temperature was increased beyond 350 °C, all four networks showed the sign of thermal decomposition by the sequential loss of carboxylic acid groups. DSC analyses strongly supported the TGA findings by displaying broad exothermic features for the loss of coordinated and lattice water molecules. The thermal stabilities of networks **3–6** were further supported by the XRPD analysis. The XRPD patterns of the activated networks (up to 300 °C) were nearly identical to those of as-synthesized samples, indicating that the structural integrity is retained even after the loss of coordinated and lattice water molecules (Figures S13–S16, SI).

■ SORPTION AND INCLUSION PROPERTIES

In addition to thermal stability, it is also desirable to evaluate the feasibility of the substrates and/or reagents to freely diffuse through the pores and channels of a network. Therefore, several sorption and inclusion studies were carried out. Gas sorption–desorption studies typically provide information about the porous nature of a network. However, the N₂ sorption analysis for all networks at 77 K showed negligible uptake (Figures S17–S18 and Table S5, SI). The Langmuir and BET surface area for all four networks were between 2.0–5.5 m² g⁻¹. These studies revealed an essentially nonporous material compared to well-established highly porous MOFs.¹⁸ The results suggest that a significant available space is being occupied by the Co³⁺-based building blocks themselves. Such an observation has been noted for our earlier metalloligand-based networks^{6e,f} as well as for other metalloligand-based materials.¹⁹ Therefore, we attempted to understand possible diffusion as well as inclusion of the reagents and/or substrates within the pores and channels of the present networks. For such investigation, combined FTIR spectral and thermal (TGA and DSC) studies were carried out for all four networks. Benzaldehyde (substrate; molecular size: 8.21 × 5.83 Å²),²⁰ aniline (reagent; molecular size: 7.44 × 5.83 Å²),²⁰ and (CH₃)₃SiCN (reagent; molecular size: 7.32 × 6.48 Å²)²⁰ were selected for their distinct FTIR spectral features. Thus, when networks **3–6** were impregnated with a CH₂Cl₂ solution containing the aforementioned reagents and/or substrates, noticeable differences were observed when compared to neat sample (see Tables S6 and S7, Supporting Information). For example, ν_{C=O} stretch for the impregnated benzaldehyde was red-shifted by 12–17 cm⁻¹ for all four networks. Similarly, the ν_{CN} stretch for the impregnated (CH₃)₃SiCN was found to red-shift by 16–21 cm⁻¹ for all four networks. A somewhat similar observation was noted for aniline-impregnated samples. Therefore, these experiments suggest that the reagents and/or

Table 3. Ring-Opening Reactions of Cyclohexene Oxide with Aniline, Para-Substituted Anilines, and Aliphatic Amines Using Catalysts 3, 4, 5, and 6



Entry ^a	Amine	Product	Yield (%) ^b			
			3	4	5	6
1			95, 94 ^c , 92 ^d	93, 91 ^c , 90 ^d	99, 98 ^c , 96 ^d	99, 96 ^c , 95 ^d
2			98	94	77	98
3			60	69	52	95
4			98	98	94	90
5			>99	98	95	>99
6			48	43	46	53

^aConditions: catalyst-2 mol %; 4 h stirring, room temperature. ^bYield calculated from the gas chromatography using internal standard. ^{c,d}Isolated yield after third and fifth run, respectively.

substrates not only have diffused but also got activated within the microporous network. Importantly, diffusion and the probable inclusion of these reagents and/or substrates caused significant perturbation to the $\nu_{\text{O-H}}$ stretches of the coordinated/lattice water molecules (see Figures S19–S22, Supporting Information). More importantly, these results are supported by the TGA and DSC studies which showed the weight loss for the impregnated reagent/substrate in addition to the coordinated/lattice water molecules. On average, weight loss of two molecules of reagent and/or substrate (benzaldehyde or $(\text{CH}_3)_3\text{SiCN}$ or aniline) was observed from the TGA/DSC studies after replacing 4–11 water molecules. Table S7 and Figures S19–S22 (Supporting Information) provide a detailed account about the thermal behavior of impregnated samples. In essence, thermal studies further support the diffusion and possible entrapment of reagent/substrate within the network. It is important to note that networks 4 and 6 are layered materials, and a possibility always exists of intercalation of substrate/reagent within the layers. Such a situation is also likely to show change in the stretching frequencies of the substrate/reagent.

A ^1H NMR based inclusion experiment²¹ was carried out to ascertain the coexistence of both substrate and reagent within the microporous network and their reaction within the confined environment. Therefore, ROR of styrene oxide with aniline was performed as a prototype example using network 3 as the catalyst. The network 3 was impregnated with a 1:1 mixture of

styrene oxide and aniline and investigated after digesting the sample (using 1N aqueous HCl solution and extracting the products into CH_2Cl_2) at the following intervals: first at 2 h; second at 4 h; and finally at 12 h. The ^1H NMR results at 2 h display the peaks both for substrate + reagent (styrene oxide and aniline) as well as the ring-opened product (Figure S23, SI). Notably, after 12 h, the peaks corresponding to substrate and reagent were negligible, while product formation was almost quantitative while the reaction showed ca. 80% completion after 4 h. This experiment provides additional evidence that the catalysis is occurring within the microporous network.

■ APPLICATION OF $\{\text{CO}^{3+}\text{-Zn}^{2+}\}$ AND $\{\text{CO}^{3+}\text{-Cd}^{2+}\}$ NETWORKS IN HETEROGENEOUS CATALYSIS

The Lewis acidic nature of secondary Zn^{2+} and Cd^{2+} metal ions, presence of labile water molecules, and their displacement with substrate/reagent as revealed by inclusion studies; availability of well-defined pores and channels; and their ability to entrap substrate/reagent in our heterobimetallic networks depicted the likelihood of catalysis within the microporous networks. Keeping these points in perspective, we narrowed down to catalytic reactions where the substrates are oxygen-based (for ease in displacing the water molecules), and the reactions are known to be catalyzed by the Lewis acidic metal ions. The RORs of epoxides and cyanation reactions (CRs) of aldehydes were appeared to be the most suitable choices considering the

Table 4. Ring-Opening Reactions of Styrene Oxide with Aniline, Para-Substituted Anilines, and Aliphatic Amines Using Catalysts 3, 4, 5, and 6

Entry ^a	Amine	Product	Yield (%) ^b			
			3	4	5	6
1			82, 81 ^c , 80 ^d	91, 90 ^c , 90 ^d	85, 83 ^c , 82 ^d	70, 69 ^c , 68 ^d
2			96	>99	77	87
3			85	80	82	95
4			89	>99	>99	>99
5			95	97	97	98
6			83	78	82	72

^aConditions: catalyst-2 mol %; 4 h stirring, room temperature. ^bYield calculated from the gas chromatography using internal standard. ^{c,d}Isolated yield after third and fifth run, respectively.

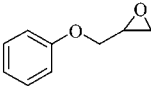
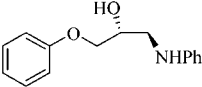
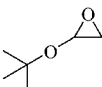
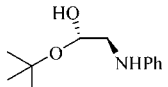
forementioned facts.^{6g} Of course, the potential heterogeneous catalytic activity of networks 3–6 was considered to be an additional benefit due to their insoluble nature and thus maintenance of structural integrity during catalysis.

Ring-Opening Reactions. RORs of epoxides with assorted amine provide an important synthetic route for the synthesis of β -amino alcohols of pharmaceutical and biological importance.²² Networks 3–6 were investigated as the heterogeneous catalysts for the aminolysis reaction under solvent-free conditions. Therefore, for the aminolysis reaction, an equimolar mixture of cyclohexene oxide and aniline was stirred at ambient temperature in the presence of only 2 mol % powdered network 3, 4, 5, or 6. Under these conditions, a smooth reaction resulted that produced the corresponding β -amino alcohol in high yield. As shown in Table 3, the networks 3–6 could promote the reaction between cyclohexene oxide with aniline (entry 1), *para*-substituted anilines (entries 2–3), as well as aliphatic amines (entries 4–6). In the absence of networks 3–6, the reaction did not proceed at all, thereby supporting the possible Lewis acidic catalyzed activity of the networks. Further, when the catalyst was filtered off, the reaction was no longer promoted. Furthermore, a control experiment of using building block 1 or 2 as the catalyst did not result in any product formation. Finally, control experiments using powdered metal salts ($\text{Zn}(\text{OAc})_2 \cdot 2\text{H}_2\text{O}$ or $\text{Cd}(\text{OAc})_2 \cdot 2\text{H}_2\text{O}$) as the catalyst resulted in very little conversion (see Table S8, SI). These control experiments clearly

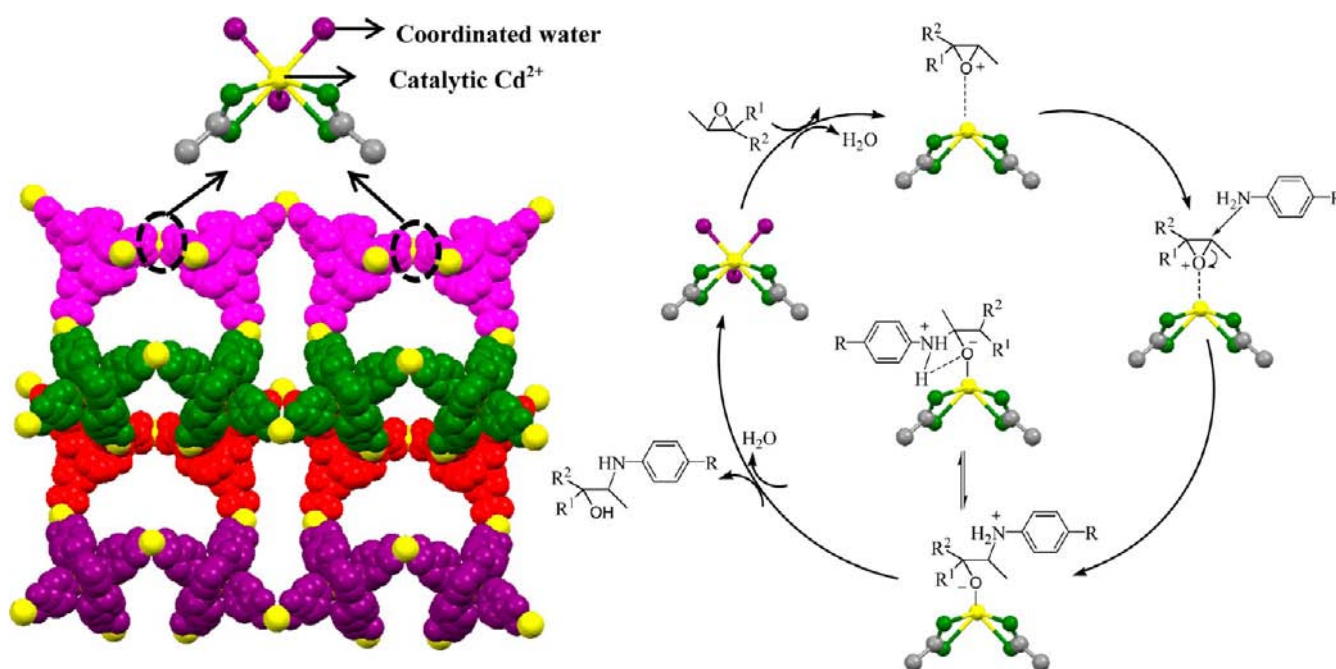
demonstrate that the soluble and catalytic active species are not leached out from networks 3–6 under the employed reaction conditions. Thus, these experiments strongly support that networks 3–6 are acting as the true heterogeneous catalysts. In addition, the heterogeneous catalysts can be conveniently recovered from the reaction mixture by simple filtration and used several times (tested five consecutive times; entry 1, Table 3) without much loss in the catalytic efficiency (3% drop in isolated yield in the fifth run). Moreover, there was no requirement of any further purification or regeneration of any of the catalysts. The FTIR and XRPD data showed that the crystallinity and structural integrity of the recovered catalysts are preserved after the catalytic reaction. A comparison of XRPD patterns of the freshly prepared and reused catalysts unambiguously supports this observation (Figures S24–S27, SI).

In order to explore the effect of electronic substituents on product yield, electron-donating and electron-withdrawing groups were placed at the *para*-position of aniline ring. As expected, the yield was higher with electron-rich aniline (entry 2) due to the better nucleophilicity than the one with electron-deficient aniline (entry 3). Moreover, aliphatic amines such as piperidine, pyrrolidine, and cyclohexyl amine were used to compare the nucleophilicity toward RORs. It was found that the yields were much better in the case of cyclic aliphatic amines (entry 4–5, Table 3) as compared to aromatic amines (entry 1–3, Table 3). A similar observation has been noted in the

Table 5. Regio-Selective Ring-Opening Reactions of Few Epoxides with Aniline Using Catalysts 3, 4, 5, and 6

Entry ^a	Epoxide	Product	Yield (%) ^b			
			3	4	5	6
1			98	86	90	82
2			97	83	86	85

^aConditions: catalyst-2 mol %; 4 h stirring, room temperature. ^bYields calculated from the gas chromatography using internal standard.

Scheme 2. Proposed Reaction Mechanism for the Ring-Opening Reaction of Asymmetrical Epoxides with Aniline Catalyzed by the Networks^a

^aA representative network 5 has been shown to display the catalytic Cd^{2+} ions (yellow spheres) located within the microporous network.


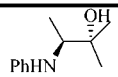

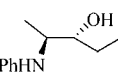
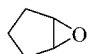
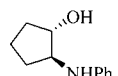
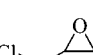
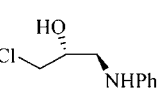
literature.²³ Importantly, the stereoselective trans product was exclusively produced in all cases without any observation of the cis product.²⁴

To probe the regioselectivity, an asymmetrical substrate styrene oxide was selected and treated with aniline, substituted anilines, cyclic aliphatic amines, or cyclohexyl amine (Table 4). Interestingly, a perfect regioselectivity was observed that resulted in only a single product in each case with all four catalysts. Out of two possible products due to the nucleophilic attack either at the benzylic carbon atom or at the less hindered carbon atom of the epoxide ring, in all cases, the nucleophilic attack exclusively took place at the benzylic carbon atom of epoxide.²⁵ The regio-isomer formed by the reaction of aniline at the benzylic carbon atom of epoxide ring showed the characteristic molecular ion peak $[\text{M}^+ - 31]$ due to the loss of CH_2OH fragment in GC-MS studies.²⁵ There are two probable reasons for the observed regioselectivity. First, confinement of the catalytic metal centers within the microporous network allows a substrate to approach in rather limited or unique orientation, thus inducing the selectivity (metal-based selectivity). Second, the positive charge on oxygen

atom appears to be localized on the highly substituted benzylic carbon leading to a single product (electronic selectivity). Therefore, it became essential to perform additional experiments to rule out one of the two possibilities.

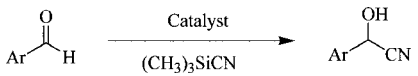
Consequently, to further establish the regioselectivity, RORs of glycidic ethers, 2-(phoxymethyl)oxirane, and 2-*tert*-butoxyoxirane with aniline were carried out (Table 5). In each case, excellent regioselectivity was noticed due to the observation of a single product. Therefore, the nucleophile exclusively attacked the less hindered side of the epoxide ring.²⁵ We reason that in the absence of a resonance effect (as the prevailing cause in the case of styrene epoxide) the regioselectivity is controlled by the steric factor, and the nucleophilic attack selectively took place at the less substituted/terminal carbon atom of the epoxide ring. The results are complementary to that of styrene epoxide and support the first hypothesis that the confinement of catalytic metal center within the microporous network is the *key-factor* in controlling the regioselectivity. On the basis of observed selectivity, a mechanism has been proposed and presented in Scheme 2.

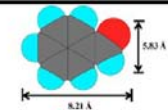
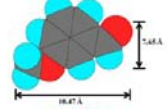
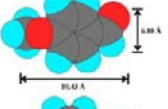
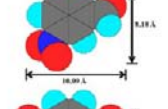
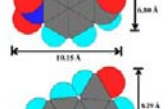
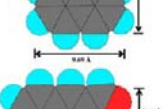
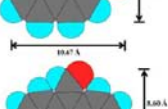
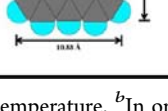
Table 6. Ring-Opening Reactions of Assorted Epoxides with Aniline Using Catalysts 3, 4, 5, and 6

Entry ^a	Epoxide	Product	Yield (%) ^b			
			3	4	5	6
1			38	42	40	55
2			62	50	35	40
3			92	90	80	85
4			78	74	86	76

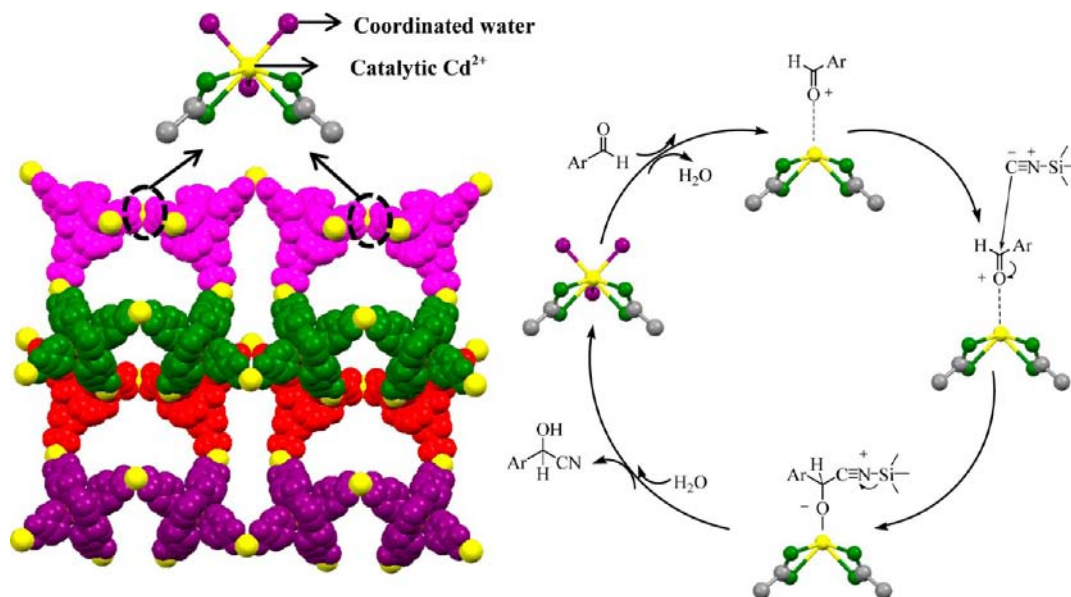
^aConditions: catalyst-2 mol %; 48 h stirring, room temperature. ^bYields calculated from the gas chromatography using internal standard.

Table 7. Cyanation Reaction of Various Aldehydes with Trimethylsilyl Cyanide Using Catalysts 3, 4, 5, and 6



Entry ^a	Ar	Molecular size ^b	Yield (%) ^c			
			3	4	5	6
1	Ph		90	94	86	92
2	3-MeOC ₆ H ₄		80	76	80	82
3	4-MeOC ₆ H ₄		71	60	69	81
4	3-NO ₂ C ₆ H ₄		90	86	90	76
5	4-NO ₂ C ₆ H ₄		95	92	90	85
6	1-Naphthyl		98	71	68	70
7	2-Naphthyl		98	60	60	64
8	9-Anthracenyl		43	40	38	52

^aConditions: catalyst-5 mol %; 4 h stirring, room temperature. ^bIn order to measure the dimension of the mentioned molecule, two suitable atoms were selected and their center-to-center distance was measured by Chem3D followed by the addition of their van der Waals radii. ^cYields calculated from the gas chromatography using internal standard.

Scheme 3. Proposed Reaction Mechanism for the Cyanation Reaction of Aldehydes with TMSCN Catalyzed by the Networks^a

^aA representative network 5 has been shown to display the catalytic Cd^{2+} ions (yellow spheres) located within the microporous network.

To understand the effect of steric crowding on the reactivity and selectivity in our catalytic systems, we conducted the aminolysis of 2,3-epoxypentane and 2,3-epoxy-2-methylbutane with aniline (entries 1 and 2, Table 6).²⁶ Interestingly, for both these epoxides, the nucleophilic attack predominantly occurred on the less hindered carbon atom. The major products (>95%) were *N*-phenylamino-3-pentenol and 2-methyl-3-phenylamino-butane-2-ol for the former and latter substrates, respectively.²⁶ These results suggest that the epoxide ring has interacted with the catalytic metal ions through the less-hindered side, possibly due to steric reasons caused by the attached arylcarboxylic acid rings and solvent molecules. The catalytic metal ion is capable of distinguishing between a methyl and an ethyl substituent with a high selectivity.²⁶ Notably, when nonplanar cyclohexyl amine was used as the nucleophile, poor conversions were noticed (entry 6, Tables 3 and 4) when compared to RORs with aniline (entry 1, Tables 3 and 4). The poor product yield even after prolonged reaction time (48 h) can be correlated to the hindered accessibility due to the nonplanar nature of cyclohexyl amine. Collectively, these results display the importance of accessibility to the catalytic metal ions confined within the interior of microporous network. The ring-opening of cyclopentene oxide with aniline also proceeded smoothly and a *trans* stereospecificity was observed in the respective product (entry 3, Table 6).

For a successful catalytic system, it is important that in addition to control over the regioselectivity; the catalyst also supports the chemoselectivity. Therefore, epichlorohydrin was selected as a potential substrate as it contains both an epoxide ring and a good leaving group, Cl.²⁷ The reaction of aniline with epichlorohydrin provided an excellent example of chemoselectivity yielding corresponding amino alcohol due to the nucleophilic attack at the terminal carbon atom of the epoxide moiety. No product arising from the nucleophilic displacement of the chlorine atom was observed with any of the four networks (entry 4, Table 6).

Cyanation Reactions. The cyanation of carbonyl-functionalized organic substrates provides a convenient route to cyanohydrins which are intermediates for a variety of fine chemicals and pharmaceuticals.²⁸ Because of the importance of

such intermediates, extensive research has been aimed to develop improved Lewis acid catalysts for the reaction of cyanide with aldehydes.²⁹ In this context, heterogeneous catalysts incorporating Lewis acidic sites are advantageous. Importantly, cyanation of aldehyde is comparatively far-more challenging than the cyanation of an imine group as the latter is an activated substrate. The success of networks 3–6 as the heterogeneous catalyst in RORs suggested their potential role in the cyanation reactions. Therefore, CRs of assorted aldehydes were performed in the presence of networks 3–6 using trimethylsilylcyanide (TMSCN) as the cyanide source (Table 7). The reaction produced the corresponding cyanohydrins in good yield. The observed catalysis is presumably occurring via displacement of the labile water molecules by aldehyde before its activation and reaction (Scheme 3). To demonstrate the functional group tolerance, cyanation of substituted benzaldehyde, such as *m*- and *p*-anisaldehyde; *m*- and *p*-nitrobenzaldehyde was performed. Benzaldehyde and anisaldehyde gave good product yield (entries 1–3, Table 7), whereas the electron-deficient aldehydes were equally effective with our catalytic systems (entries 4 and 5, Table 7). Importantly, all networks functioned as the heterogeneous catalysts and could be recycled several times. Notably, the application of $\text{Zn}(\text{OAc})_2$ and $\text{Cd}(\text{OAc})_2$ as the catalyst did not result in the observation of any product (Table S8, SI), while other control experiments yielded results similar to those noted for RORs.

The CRs of aldehydes were primarily targeted to understand the size-selectivity as such an observation does constitute good circumstantial evidence for the heterogeneous catalysis within the pores and channels of a network and not only on the surface. Thus, to probe the size selectivity, a few aldehydes of increasing molecular size were investigated.²⁰ Importantly, the reaction yield was found to systematically depend on the molecular size of the substrate when cyanation of sterically demanding substrates such as 1-naphthaldehyde, 2-naphthaldehyde, and 9-anthraldehyde was attempted. For network 4, the respective cyanohydrins were obtained with the yields (%) of 71, 60, and 40, respectively. As expected, the yields are poor in comparison

to benzaldehyde (94%) and follow the following order: benzaldehyde > 1-naphthaldehyde > 2-naphthaldehyde > 9-anthraldehyde. The relative substrate-size indicates that the channels of network 4 are large enough to freely allow benzaldehyde ($8.21 \times 5.83 \text{ \AA}^2$)²⁰ and similar substrates to diffuse through the pores/channels to reach the catalytic metal centers. In contrast, 1-naphthaldehyde ($9.69 \times 8.29 \text{ \AA}^2$),²⁰ 2-naphthaldehyde ($10.67 \times 7.49 \text{ \AA}^2$),²⁰ and especially 9-anthraldehyde ($10.88 \times 8.60 \text{ \AA}^2$)²⁰ are quite bulky to diffuse smoothly through the pores/channels where the catalytic sites are located. As a consequence, a poor conversion resulted. A similar trend was observed for the remaining networks. Thus, it could be concluded that the conversions are inversely proportional to the molecular size of the aldehydes, and the substrate accessibility (through pores or through intercalation) to the catalytic sites controls the catalysis outcome.³⁰

To understand the catalytic efficiency of all four networks, turnover frequency (TOF) was measured using a common substrate, 1-naphthaldehyde. TOF was continuously monitored for the entire duration of the cyanation reaction under the identical reaction conditions. Results suggest that the network 3 was the most time-efficient in consuming the substrate 1-naphthaldehyde followed by 5, whereas networks 4 and 6 were somewhat less effective although comparable to each other. A closer look to the structure of network 3 displays a unique orientation of aryl rings lining the channel. We speculate that such an arrangement assists in bringing/holding the substrate closer to the catalytic Lewis acidic metal through arene...arene ($\pi \cdots \pi$) interactions. Naturally, such interactions will be manifested more strongly with a naphthyl than with a phenyl ring (see entries 6 and 7, Table 7). However, when the anthracenyl group was involved, the substrate is too big to comfortably enter the pore/channel to access the Lewis acidic metal, and as a consequence product yield dropped dramatically.

It is important to emphasize that in all aforementioned catalytic examples all four networks provided similar catalytic results. Interestingly, despite similar structural nature, related topology, and identical coordinated solvent molecules, the four networks were expected to show certain differences. We believe that although networks 3 and 5 with *para*-arylcarboxylate groups offer an elongated network with wider pores and therefore higher substrate/reagent accessibility, the remaining two networks 4 and 6 (with *meta*-arylcarboxylate groups) are benefitted by their layered structure. Thus, there is an interesting trade-off between pore-based and intercalation-based substrate/reagent accessibility. Such an observation nicely illustrates the importance of designed material to execute as well as control a catalytic event.

CONCLUSION

In summary, we have shown few $\{\text{Co}^{3+}-\text{Zn}^{2+}\}$ and $\{\text{Co}^{3+}-\text{Cd}^{2+}\}$ heterobimetallic networks that have been synthesized using Co^{3+} complexes appended with arylcarboxylate groups as the building blocks. These examples showcase a great promise in the development of crystalline network materials with facile tunability. We showed the application of immobilized catalytically active Zn^{2+} and Cd^{2+} centers in such networks to promote heterogeneous RORs of epoxides and CRs of aldehydes. A perfect stereo- and regioselectivity was observed with asymmetrical epoxides, whereas epichlorohydrin provided an example of chemoselectivity. CRs of aldehydes have helped us in rationalizing the molecular size of the substrates to that of accessibility offered by the networks. The simple synthesis, reusability, and heterogeneous nature of these heterobimetallic

networks merit wider catalytic applications, and several such studies are in progress in the laboratory.

ASSOCIATED CONTENT

Supporting Information

X-ray crystallographic data for networks 3 and 4 in CIF format, figures for the diffuse-reflectance absorption spectra, XRPD patterns, TGA–DSC plots, sorption plots, NMR spectra, and crystal structures; and tables for sorption data, control catalytic experiments, and molecular dimensions. This material is available free of charge via the Internet at <http://pubs.acs.org>.

AUTHOR INFORMATION

Corresponding Author

*Fax: +91-11-27666605; e-mail: rgupta@chemistry.du.ac.in.

Notes

The authors declare no competing financial interest.

ACKNOWLEDGMENTS

R.G. gratefully acknowledges the financial support from the Department of Science and Technology (DST), Govt. of India, New Delhi. Crystallographic data and analytical facilities were provided by the CIF-USIC facility of this university. Authors thank AIRF-JNU for GC and GC–MS studies and Dr. R. Nagarajan for PXRD data. G.K. thanks CSIR for the award of SRF. Reviewers' comments were very helpful at the revision stage.

REFERENCES

- (1) (a) Fujita, M.; Tominaga, M.; Hori, A.; Therrien, B. *Acc. Chem. Res.* **2005**, *38*, 369. (b) O'Keeffe, M.; Yaghi, O. M. *Chem. Rev.* **2012**, *112*, 675. (c) Chkrabarty, R.; Mukherjee, P. S.; Stang, P. J. *Chem. Rev.* **2011**, *111*, 6810. (d) Gu, X.; Lua, Z. H.; Xu, Q. *Chem. Commun.* **2010**, *46*, 7400.
- (2) (a) Sun, Y. Q.; Zhang, J.; Chen, Y. M.; Yang, G. Y. *Angew. Chem., Int. Ed.* **2005**, *44*, 5814. (b) Zhong, D. C.; Meng, M.; Zhu, J.; Yang, G. Y.; Lu, T. B. *Chem. Commun.* **2010**, *46*, 4354. (c) Wang, Z.; Cohen, S. M. *J. Am. Chem. Soc.* **2007**, *129*, 12368. (d) Halper, S. R.; Cohen, S. M. *Inorg. Chem.* **2005**, *44*, 4139. (e) Halper, S. R.; Cohen, S. M. *Inorg. Chem.* **2005**, *44*, 486. (f) Halper, S. R.; Do, L.; Stork, J. R.; Cohen, S. M. *J. Am. Chem. Soc.* **2006**, *128*, 15255. (g) Murphy, D. L.; Malachowski, M. R.; Campana, C. F.; Cohen, S. M. *Chem. Commun.* **2005**, 5506. (h) Halper, S. R.; Cohen, S. M. *Chem.—Eur. J.* **2003**, *9*, 4661. (i) Halper, S. R.; Cohen, S. M. *Angew. Chem., Int. Ed.* **2004**, *43*, 2385. (j) Garibay, S. J.; Stork, J. R.; Wang, Z.; Cohen, S. M.; Telfer, S. G. *Chem. Commun.* **2007**, 4881. (k) Chen, B.; Fronczek, F. R.; Maverick, A. W. *Inorg. Chem.* **2004**, *43*, 8209. (l) Chen, B.; Fronczek, F. R.; Maverick, A. W. *Chem. Commun.* **2003**, 2166. (m) Zhang, Y.; Chen, B.; Fronczek, F. R.; Maverick, A. W. *Inorg. Chem.* **2008**, *47*, 4433. (n) Vreshch, V. D.; Chernega, A. N.; Howard, J. A. K.; Sieler, J.; Domasevitch, K. V. *Dalton Trans.* **2003**, 1707. (o) Vreshch, V. D.; Lysenko, A. B.; Chernega, A. N.; Howard, J. A. K.; Krautscheid, H.; Sieler, J.; Domasevitch, K. V. *Dalton Trans.* **2004**, 2899.
- (3) (a) Ma, L.; Abney, C.; Lin, W. *Chem. Soc. Rev.* **2009**, *38*, 1248. (b) Lee, J.; Farha, O. K.; Roberts, J.; Scheidt, K. A.; Nguyen, S. T.; Hupp, J. T. *Chem. Soc. Rev.* **2009**, *38*, 1450. (c) Corma, A.; Garcia, H.; Xamena, F. X. L. *Chem. Rev.* **2010**, *110*, 4606.
- (4) Farha, O. K.; Malliakas, C. D.; Kanatzidis, M. G.; Hupp, J. T. *J. Am. Chem. Soc.* **2010**, *132*, 950 and references cited therein.
- (5) (a) Ali, A.; Hundal, G.; Gupta, R. *Cryst. Growth Des.* **2012**, *12*, 1308. (b) Kumar, G.; Aggarwal, H.; Gupta, R. *Cryst. Growth Des.* **2013**, *13*, 74.
- (6) (a) Mishra, A.; Ali, A.; Upreti, S.; Gupta, R. *Inorg. Chem.* **2008**, *47*, 154. (b) Mishra, A.; Ali, A.; Upreti, S.; Whittingham, M. S.; Gupta, R. *Inorg. Chem.* **2009**, *48*, 5234. (c) Singh, A. P.; Gupta, R. *Eur. J. Inorg. Chem.* **2010**, 4546. (d) Kumar, G.; Singh, A. P.; Gupta, R. *Eur. J. Inorg. Chem.* **2010**, 5103. (e) Singh, A. P.; Ali, A.; Gupta, R. *Dalton Trans.* **2010**, 39, 8135. (f) Singh, A. P.; Kumar, G.; Gupta, R. *Dalton Trans.* **2011**, *40*, 12454. (g) Kumar, G.; Gupta, R. *Inorg. Chem.* **2012**, *51*, 5497.

- (7) (a) Li, H.; Eddaoudi, M.; Groy, T. L.; Yaghi, O. M. *J. Am. Chem. Soc.* **1998**, *120*, 8571. (b) Li, H.; Eddaoudi, M.; O'Keeffe, M.; Yaghi, O. M. *Nature* **1999**, *402*, 276. (c) Kondo, M.; Yoshitomi, T.; Seki, K.; Matsuzaka, H.; Kitagawa, S. *Angew. Chem., Int. Ed. Engl.* **1997**, *36*, 1725. (d) Serre, C.; Férey, G. *Inorg. Chem.* **1999**, *38*, 5370. (e) Hirai, K.; Furukawa, S.; Kondo, M.; Uehara, H.; Hiromitsu, S.; Sakata, O.; Kitagawa, S. *Angew. Chem., Int. Ed.* **2011**, *50*, 8057. (f) Stock, N.; Biswas, S. *Chem. Rev.* **2012**, *112*, 933. (g) Zou, R. Q.; Zhong, R. Q.; Du, M.; Pandey, D. S.; Xu, Q. *Cryst. Growth Des.* **2008**, *8*, 452.
- (8) (a) Chen, B.; Eddaoudi, M.; Hyde, S. T.; O'Keeffe, M.; Yaghi, O. M. *Science* **2001**, *291*, 1021. (b) Rowsell, L. C.; Yaghi, O. M. *Angew. Chem., Int. Ed.* **2005**, *44*, 4670. (c) Spencer, E. C.; Howard, J. A. K.; McIntyre, G. J.; Rowsell, J. L. C.; Yaghi, O. M. *Chem. Commun.* **2006**, 278. (d) Zhong, R. Q.; Zou, R. Q.; Du, M.; Yamada, T.; Maruta, G.; Takeda, S.; Lid, J.; Xu, Q. *CrystEngComm* **2010**, *12*, 677. (e) Doonan, C. J.; Tranchemontagne, D. J.; Glover, T. G.; Hunt, J. R.; Yaghi, O. M. *Nat. Chem.* **2010**, *2*, 235. (f) Han, D.; Jiang, F.-L.; Wu, M.-Y.; Chen, L.; Hong, M.-C. *Chem. Commun.* **2011**, 9861. (g) Suh, M. P.; Park, H. J.; Prasad, T. K.; Lim, D.-W. *Chem. Rev.* **2012**, *112*, 782. (h) Getman, R. B.; Bae, Y.-S.; Wilmur, R. C. E.; Snurr, Q. *Chem. Rev.* **2012**, *112*, 703.
- (9) (a) Lee, C. Y.; Farha, O. K.; Hong, B. J.; Sarjeant, A. A.; Nguyen, S. T.; Hupp, J. T. *J. Am. Chem. Soc.* **2011**, *133*, 15858. (b) Kent, C. A.; Liu, D.; Ma, L.; Papanikolas, J. M.; Meyer, T. J.; Lin, W. *J. Am. Chem. Soc.* **2011**, *133*, 12940.
- (10) (a) Seo, J. S.; Whang, D.; Lee, H.; Jun, S. I.; Oh, J.; Jeon, Y. J.; Kim, K. *Nature* **2000**, *404*, 982. (b) Xamena, F. X. L.; Abad, A.; Corma, A.; Garcia, H. *J. Catal.* **2007**, *250*, 294. (c) Ye, J.-Y.; Liu, C.-J. *Chem. Commun.* **2011**, 47, 2167. (d) Cohen, S. *Chem. Rev.* **2012**, *112*, 470. (e) Yoon, M.; Srirambalaji, R.; Kim, K. *Chem. Rev.* **2012**, *112*, 1196. (f) Jiang, H. L.; Xu, Q. *Chem. Commun.* **2011**, 47, 3351. (g) Gu, X.; Lu, Z. H.; Jiang, H. L.; Akita, T.; Xu, Q. *J. Am. Chem. Soc.* **2011**, *133*, 11822.
- (11) (a) Jeong, N. C.; Samanta, B.; Lee, C. Y.; Farha, O. K.; Hupp, J. T. *J. Am. Chem. Soc.* **2012**, *134*, 51. (b) Taylor, J. M.; Mah, R. K.; Ratcliffe, C. I.; Moudrakovski, I.; Vaidhyanathan, R.; Shimizu, G. K. H. *J. Am. Chem. Soc.* **2010**, *132*, 14055. (c) Hurd, J. A.; Vaidhyanathan, R.; Thangadurai, V.; Ratcliffe, C. I.; Moudrakovski, I. L.; Shimizu, G. K. H. *Nat. Chem.* **2009**, *1*, 705.
- (12) Kreno, L. E.; Leong, K.; Farha, O. K.; Allendorf, M.; Van Duyne, R. P.; Hupp, J. T. *Chem. Rev.* **2012**, *112*, 1105.
- (13) (a) Zhao, H.; Jin, Z.; Su, H.; Jing, X.; Sun, F.; Zhu, G. *Chem. Commun.* **2011**, 47, 6389. (b) Horcajada, P.; Serre, C.; Maurin, G.; Ramsahye, N. A.; Balas, F.; Vallet-Regí, M.; Sebban, M.; Taulelle, F.; Férey, G. *J. Am. Chem. Soc.* **2008**, *130*, 6774. (c) Della Rocca, J.; Liu, D.; Lin, W. *Acc. Chem. Res.* **2011**, *44*, 957. (d) Horcajada, P.; Gref, R.; Baati, T.; Allen, P. K.; Maurin, G.; Couvreur, P.; Férey, G.; Morris, R. E.; Serre, C. *Chem. Rev.* **2012**, *112*, 1232.
- (14) (a) He, J.; Xu, Z.; Zeller, M.; Hunter, A. D. *J. Am. Chem. Soc.* **2012**, *134*, 1553. (b) Gole, B.; Bar, A. K.; Mukherjee, P. S. *Chem. Commun.* **2011**, 12137. (c) Wanderley, M. M.; Wang, C.; Wu, C.-D.; Lin, W. *J. Am. Chem. Soc.* **2012**, *134*, 9050. (d) Sapchenko, S. A.; Samsonenko, D. G.; Dybtsev, D. N.; Melgunov, M. S.; Fedin, V. P. *Dalton Trans.* **2011**, 40, 2196. (e) Zhan, C.-H.; Wang, F.; Kang, Y.; Zhang, J. *Inorg. Chem.* **2012**, *51*, 523. (f) Wang, H.-N.; Meng, X.; Qin, C.; Wang, X.-L.; Yang, G.-S.; Su, Z.-M. *Dalton Trans.* **2012**, 41, 1047. (g) Ciu, Y.; Yue, Y.; Qian, G.; Chen, B. *Chem. Rev.* **2012**, *112*, 1126. (h) Wang, H.; Zhu, G. *Adv. Mater. Res.* **2012**, *345*, 245.
- (15) (a) Perrin, D. D.; Armarego, W. L. F.; Perrin, D. R. *Purification of Laboratory Chemicals*; Pergamon Press: Oxford, 1980. (b) Nakamoto, K. *Infrared and Raman Spectra of Inorganic and Coordination Compounds*; Wiley: New York, 1997.
- (16) (a) Kim, J.; Chen, B.; Reineke, T. M.; Li, H.; Eddaoudi, M.; Moler, D. B.; O'Keeffe, M.; Yaghi, O. M. *J. Am. Chem. Soc.* **2001**, *123*, 8239. (b) Tranchemontagne, D. J.; Mendoza-Corté, J. L.; O'Keeffe, M.; Yaghi, O. M. *Chem. Soc. Rev.* **2009**, *38*, 1257. (c) Shin, J. W.; Bae, J. M.; Kim, C.; Min, K. S. *Inorg. Chem.* **2013**, *52*, 2265.
- (17) (a) Gu, J.-M.; Kwon, T.-H.; Park, J.-H.; Huh, S. *Dalton Trans.* **2010**, 39, S608. (b) Gu, J.-M.; Kim, W.-S.; Huh, S. *Dalton Trans.* **2011**, 40, 10826. (c) Lin, X.-M.; Li, T.-T.; Chen, L.-F.; Zhang, L.; Su, C.-Y. *Dalton Trans.* **2012**, 41, 10422.
- (18) (a) Yaghi, O. M.; Li, H.; Davis, C.; Richardson, D.; Groy, T. L. *Acc. Chem. Res.* **1998**, *31*, 474. (b) Ren, T. D.; Sarkisov, L.; Yaghi, O. M.; Snurr, R. Q. *Langmuir* **2004**, *20*, 2683. (c) Yaghi, O. M.; Li, H. L. *J. Am. Chem. Soc.* **1995**, *117*, 10401. (d) Rowsell, J. L. C.; Yaghi, O. M. *Microporous Mesoporous Mater.* **2004**, *73*, 3. (e) Férey, G.; Mellot-Draznieks, C.; Serre, C.; Millange, F.; Dutour, J.; Surble, S.; Margiolaki, I. *Science* **2005**, *309*, 2040. (f) Rosi, N. L.; Eckert, J.; Eddaoudi, M.; Vodak, D. T.; Kim, J.; O'Keeffe, M.; Yaghi, O. M. *Science* **2003**, *300*, 1127.
- (19) (a) Yang, C.; Wang, X. P.; Omary, M. A. *J. Am. Chem. Soc.* **2007**, *129*, 15454. (b) Kawano, M.; Kawamichi, T.; Haneda, T.; Kojima, T.; Fujita, M. *J. Am. Chem. Soc.* **2007**, *129*, 15418. (c) Hwang, I. H.; Bae, J. M.; Kim, W. S.; Jo, Y. D.; Kim, C.; Kim, Y.; Kim, S. J.; Huh, S. *Dalton Trans.* **2012**, 41, 12759.
- (20) In order to measure the dimensions of the mentioned molecule, two suitable atoms were selected and their center-to-center distance was measured by Chem3D (Chem3D Ultra 8.0, CambridgeSoft Corporation, Cambridge, MA, 2003) followed by the addition of their van der Waals radii.
- (21) Tanabe, K. K.; Cohen, S. M. *Inorg. Chem.* **2010**, *49*, 6766.
- (22) (a) Holderich, W.; Barsnick, U. In *Fine Chemicals Through Heterogeneous Catalysis*; Sheldon, R. A., van Bekkum, H.; Wiley-VCH: Weinheim, 2001. (b) Morten, C. J.; Byers, A. J.; Van Dyke, A. R.; Vilotijevic, I.; Jamison, T. F. *Chem. Soc. Rev.* **2009**, *38*, 3175. (c) Sharpless, K. B.; Verhoeven, T. R. *Aldrichim. Acta* **1979**, *12*, 63. For MOF-based catalysts, see (d) Fujita, M.; Kwon, Y. J.; Washizu, S.; Ogura, K. *J. Am. Chem. Soc.* **1994**, *116*, 1151. (e) Ohmori, O.; Fujita, M. *Chem. Commun.* **2004**, 1586. (f) Wu, C.-D.; Hu, A.; Zhang, L.; Lin, W. *J. Am. Chem. Soc.* **2005**, *127*, 8940. (g) Tanaka, K.; Oda, S.; Shiro, M. *Chem. Commun.* **2008**, 820. (h) Park, J.; Lang, K.; Abboud, K. A.; Hong, S. *J. Am. Chem. Soc.* **2008**, *130*, 16484. (i) Lee, S. J.; Lin, W. *J. Am. Chem. Soc.* **2002**, *124*, 4554. (j) Dewa, T.; Saiki, T.; Aoyama, Y. *J. Am. Chem. Soc.* **2001**, *123*, 502. (k) Endo, K.; Koike, T.; Sawaki, T.; Hayashida, O.; Masuda, H.; Aoyama, Y. *J. Am. Chem. Soc.* **1997**, *119*, 4117. (l) Evans, O. R.; Ngo, H. L.; Lin, W. *J. Am. Chem. Soc.* **2001**, *123*, 10395. (m) Gomez-Lor, B.; Gutierrez-Puebla, E.; Iglesias, M.; Monge, M. A.; Ruiz-Valero, C.; Snejko, N. *Inorg. Chem.* **2002**, *41*, 2429.
- (23) Mancillia, G.; Femenia-Rios, M.; Macias-Sanchez, A. J.; Collado, I. G. *Tetrahedron* **2008**, *64*, 11732.
- (24) (a) Arai, K.; Lucarini, S.; Salter, M. M.; Ohta, K.; Yamashita, Y.; Kobayashi, S. *J. Am. Chem. Soc.* **2007**, *129*, 8103. (b) Liu, Z. Q.; Fan, Y.; Li, R.; Zhou, B.; Wu, L. M. *Tetrahedron Lett.* **2005**, *46*, 1023.
- (25) Shivani, Pujala, B.; Chakraborti, A. K. *J. Org. Chem.* **2007**, *72*, 3713.
- (26) (a) Desai, H.; D'Souza, B. R.; Foether, D.; Johnson, B. F.; Lindsay, H. A. *Synthesis* **2007**, 902. (b) Arai, K.; Salter, M. M.; Yamashita, Y.; Kobayashi, S. *Angew. Chem., Int. Ed.* **2007**, *46*, 955.
- (27) (a) Shivani, Chakraborti, A. K. *J. Mol. Catal. A: Chem.* **2007**, *263*, 137. (b) Chakraborti, A. K.; Kondaskar, A.; Rudrawar, S. *Tetrahedron* **2004**, *60*, 9085.
- (28) (a) Muller, U.; Schubert, M. M.; Yaghi, O. M. In *Handbook of Heterogeneous Catalysis*; Ertl, G.; Knozinger, H.; Schuth, F.; Weitkamp, J., Eds.; Wiley-VCH: Weinheim, Germany, 2008. (b) Gregory, R. J. H. *Chem. Rev.* **1999**, *99*, 3649. (c) North, M. *Tetrahedron: Asymmetry* **2003**, *14*, 147. (d) Brunel, J. M.; Holmes, I. P. *Angew. Chem., Int. Ed.* **2004**, *43*, 2752.
- (29) (a) Ryu, D. H.; Corey, E. J. *J. Am. Chem. Soc.* **2004**, *126*, 8106. (b) Keith, J. M.; Jacobsen, E. N. *Org. Lett.* **2004**, *6*, 153. (c) Hamashima, Y.; Sawada, D.; Kanai, M.; Shibasaki, M. *J. Am. Chem. Soc.* **1999**, *121*, 2641. (d) Hamashima, Y.; Kanai, M.; Shibasaki, M. *Tetrahedron Lett.* **2001**, *42*, 691. (e) Masumoto, S.; Yabu, K.; Kanai, M.; Shibasaki, M. *Tetrahedron Lett.* **2002**, *43*, 2919. (f) Hamashima, Y.; Kanai, M.; Shibasaki, M. *J. Am. Chem. Soc.* **2000**, *122*, 7412. (g) Baleizao, C.; Gigante, B.; Garcia, H.; Corma, A. *Tetrahedron Lett.* **2003**, *44*, 6813. (h) Baleizao, C.; Gigante, B.; Garcia, H.; Corma, A. *Green Chem.* **2002**, *4*, 272. (i) Mori, M.; Imma, H.; Nakai, T. *Tetrahedron Lett.* **1997**, *38*, 6229.
- (30) (a) Horike, S.; Dincà, M.; Tamaki, K.; Long, J. R. *J. Am. Chem. Soc.* **2008**, *130*, 5854. (b) Meek, S. T.; Greathouse, J. A.; Allendorf, M. D. *Adv. Mater.* **2011**, *23*, 249. (c) Li, J.-R.; Sculley, J.; Zhou, H.-C. *Chem.*

Rev. **2012**, *112*, 869. (d) Gu, J. M.; Kim, W. S.; Huh, S. *Dalton Trans* **2011**, *40*, 10826.